

Fahmy M. Haggag¹, J. A. Wang², M. A. Sokolov², and K. L. Murty³

USE OF PORTABLE/*IN SITU* STRESS-STRAIN MICROPROBE SYSTEM TO MEASURE STRESS-STRAIN BEHAVIOR AND DAMAGE IN METALLIC MATERIALS AND STRUCTURES

REFERENCE: Haggag, Fahmy M., Wang, J. A., Sokolov, M. A., and Murty, K. L., "Use of Portable/*In Situ* Stress-Strain Microprobe System to Measure Stress-Strain Behavior and Damage in Metallic Materials and Structures", Nontraditional Methods of Sensing Stress, Strain, and Damage in Materials and Structures, ASTM STP 1318, G. Lucas, and D. Stubbs Eds., American Society for Testing and Materials, Philadelphia, 1997.

ABSTRACT: A novel portable/*in situ* Stress-Strain Microprobe (SSM) system was used to measure true-stress/true-plastic-strain (σ_t - ϵ_p) behavior of several metallic materials, welds, and their heat-affected-zones (HAZs) in various metallurgical and damage conditions. The SSM system utilized an automated ball indentation (ABI) technique to measure elastic modulus, yield strength, σ_t - ϵ_p curve, strength coefficient, strain-hardening-exponent (uniform ductility), and to estimate fracture toughness (from the ABI-measured flow properties) in carbon steels, stainless steels, nickel alloys, aluminum alloys, titanium alloys, zirconium alloys, etc. Numerous ABI tests were also conducted on several nuclear pressure vessel steels (NPVSSs) in the unirradiated, neutron irradiated, and post-irradiated thermally-annealed conditions. For all these test materials and conditions, the ABI-derived results were in good agreement with those from conventional standard test methods. Furthermore, the nondestructive ABI test results rigorously indicated the various levels of neutron-embrittlement damage and the percentage of ductility recovery following thermal annealing of the NPVS specimens. *In situ*/nondestructive structural applications of the SSM system and its ABI technique have been demonstrated by testing a circumferentially welded stainless steel pipe and a full-thickness section of a nuclear pressure vessel (using 90° V-blocks and magnetic mounts for temporary attachment of the SSM testing head to the pipe and the steel section, respectively). All SSM localized tests were computer-controlled and conducted in less than 2 minutes per ABI test; depending on the desired strain rate. Example test results on metallic structural components and samples are presented in this paper.

KEYWORDS: nondestructive, *in situ*, structural integrity, ball indentation, partial unloading, welds, heat affected zone, yield strength, flow properties, metals

¹President, Advanced Technology Corp., 115 Clemson Dr., Oak Ridge, TN 37830

²Research Scientist, Oak Ridge National Laboratory, Oak Ridge, TN 37831

³Professor, North Carolina State University, Raleigh, NC 27695

INTRODUCTION

A portable/*in situ* stress-strain microprobe (SSM) system was developed recently by Advanced Technology Corporation (ATC) to test minimal material and determine several mechanical properties (e.g., yield strength, flow properties, strain-hardening exponent, strength coefficient) of metallic structures including their welds and heat-affected zones. The SSM system utilizes an automated ball indentation (ABI) technique which is nondestructive and provides a localized direct measurement of the stress-strain curve at quasi-static strain rates at room temperature. The SSM system and test methods [1,2] are based on well demonstrated and accepted physical and mathematical relationships which govern metal behavior under multi axial indentation loading. A summary of the automated ball indentation (ABI) technique is given in Ref. [2] while more details are given in Refs. [3-15]. The testing head of the SSM system can be configured for ABI field and laboratory testing as well as for testing of miniature tensile test specimens. The ABI technique is based on strain-controlled multiple indentations (at a single penetration location) of a polished surface by a nonlinear-geometry indenter (tungsten carbide spherical indenters of 0.25 to 1.57-mm diameter). The indentation depth is progressively increased to a maximum user-specified limit (typically less than 15% of the indenter diameter) with innovative intermediate partial unloadings. The applied indentation loads and associated penetration depths are continuously acquired during the ABI test and used to calculate the incremental stress-strain values based on elasticity and plasticity theories and few semi-empirical equations. The ABI test is considered nondestructive since it generates a shallow spherical depression with no sharp edges or stress concentration sites. Furthermore, the compressive residual stress left in the ABI test area retards crack initiation.

The microprobe system currently utilizes an electro-mechanically-driven indenter, high resolution penetration transducer and load cell, a personal computer (PC), a 16-bit data acquisition/control unit, and copyrighted ABI software. Automation of the test, where a PC and a test controller were used in innovative ways to control the test (including a real-time graphics and digital display of load-depth test data) as well as to analyze test data (including tabulated summary and macro-generated plots), made it accurate and highly reproducible. Results of ABI tests (at several strain rates) on various base metals, welds, and heat-affected-zones (HAZs), at different metallurgical conditions are presented and discussed in this paper. Excellent agreement was obtained between ABI-derived data and those from conventional ASTM methods. Gradients in the yield strength and flow properties and correlations to the material microstructure in the weld and HAZ areas are discussed in Ref. [8]. A 347 stainless steel (SS) flat specimen was also tested and the ABI results compared to its material certification. *In situ* SSM configuration (Fig. 1) was used successfully to test a 100-mm outer diameter 347 SS pipe containing a circumferential weld. New SSM applications on welds, HAZs, neutron-irradiated, and thermally-annealed steels are presented in this paper.

PORTABLE/*IN SITU* STRESS-STRAIN MICROPROBE SYSTEM AND ABI TESTING

Figure 1 shows the different components of microprobe system used in this work. These include: 1) a compact testing head, shown here in its *in situ* field configuration 2) a

small electronics cabinet which contains the data acquisition/control unit, other boards for signal conditioning and control, and the drive of the servo motor, and 3) a portable personal computer. Other testing head mounts such as magnetic holders were successfully used.



FIG. 1--A portable Stress-Strain Microprobe (SSM) system is used here for *in situ* testing of circumferentially welded type 347 stainless steel pipe (100 mm outer diameter and 5 mm thick). The pipe is held in a wooden stand to demonstrate this field application of the SSM system. Four aluminum V-blocks were used to temporarily attach the testing head (two column load frame) of the microprobe system to the pipe, allowing a 360° inspection of the stress-strain curve gradients in the weld and its HAZ. The inset photo is an enlargement of the 100 mm pipe, chuck (20 mm diameter) holding a 1.57 mm spherical tip indenter, and a displacement transducer mounted in a horizontal bracket. (The bench-top system, which is not shown here, has a support platen for laboratory specimen testing.)

ABI DATA ANALYSIS

Yield Strength Determination from an ABI Test

In a tensile test the uniaxial deformation is usually contained in the constant volume of the specimen's gage section. Hence, after the completion of elastic/linear loading of a metallic specimen, plastic-yielding and work-hardening commence and continue until necking occurs. In contrast, in an ABI test the elastic and plastic deformation are not distinctively separated. With increasing indentation penetration depth, an increasing volume of test material is forced to flow under multi axial compression caused by the indenter. Thus, in an ABI test both yielding and work-hardening occur simultaneously during the entire ABI test without a definite single-yield-point (because there is no constant deformation volume in an ABI test). Consequently, an accurate determination of yield strength should be based on the entire load-displacement curve of the ABI test as explained later. It should be emphasized here that an ABI test consisting of, for example, 7

loading/unloading indentation cycles (see Fig. 2-a), there will be 7 consecutive yielding processes (of new material each time the indenter has penetrated deeper into the test material) as well as 7 consecutive processes of work hardening (of both old and new material). Hence, the yield strength analysis in ABI testing should account for this simultaneous occurrence of yielding and strain-hardening of test material under ABI multi axial compression. Details of yield strength determination from ABI tests are given elsewhere [1,2,3].

The reason for the approximately linear relation of indentation load versus depth (Fig. 2-a) is because of the dual nonlinear processes occurring in opposite directions (i.e. the nonlinear increase of load versus depth due to the spherical geometry of the ball indenter is being offset by the power-law work-hardening behavior of the metallic test material). Hence, ABI tests do not exhibit the traditional segmented behavior (linear elastic followed by nonlinear/work-hardening) of the tensile load-displacement data.

For each ABI loading cycle the total penetration depth (h_t) is measured while the load is being applied, then converted to a total indentation chordal diameter (d_t) using the following equation:

$$d_t = 2 (h_t D - h_t^2)^{0.5} \quad (1)$$

where D is the indenter diameter. Data points from all loading cycles up to $d_t/D = 1.0$ are fit by linear regression analysis to the following relationship:

$$P/d_t^2 = A (d_t/D)^{m-2} \quad (2)$$

where P is the applied indentation load, m is Meyer's coefficient, and A is a test material (or specimen) parameter obtained from the regression analysis of test data of d_t/D versus P/d_t^2 . The test material parameter (A) is then used to calculate the yield strength (σ_y) of the material using the following equation:

$$\sigma_y = \beta_m A \quad (3)$$

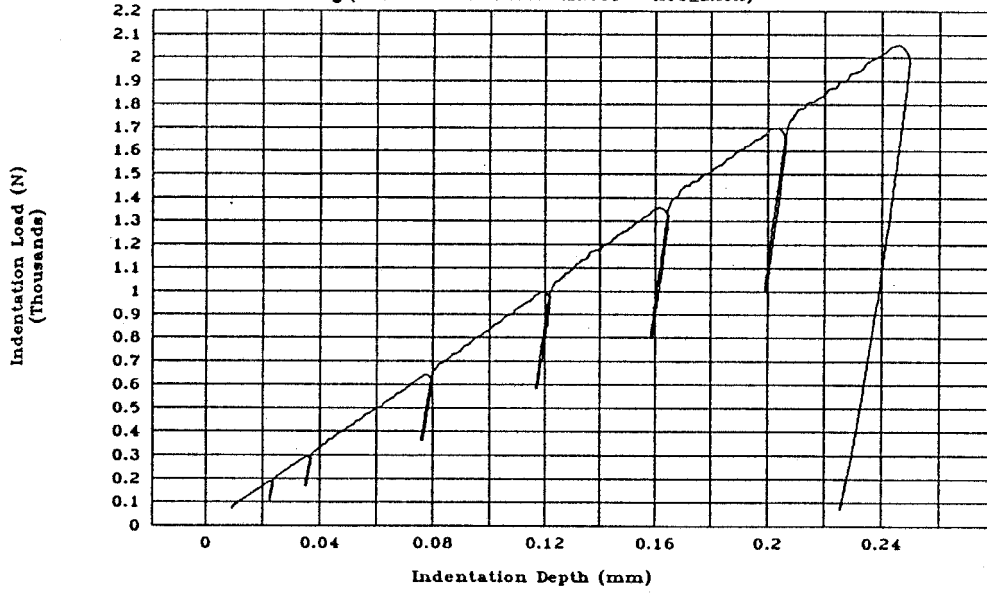
where β_m is a material-type constant (e.g., a single value of $\beta_m = 0.2285$ [2,3] is applicable to all carbon steels whether cold rolled, hot rolled, or irradiated). The value of β_m for each class or type of material is determined from regression analysis of various tensile yield-strength values (measured from specimens with different heat treatments and flow properties and machined from different orientations) and their corresponding "A" values as measured from entire ABI curves (up to $d_t/D = 1.0$). In equation 3 above, the units of A and σ_y should be the same.

Flow Properties

The homogeneous plastic flow portion of the true-stress (σ_t)/true-plastic-strain (ϵ_p)

Indentation Load-Depth Plot

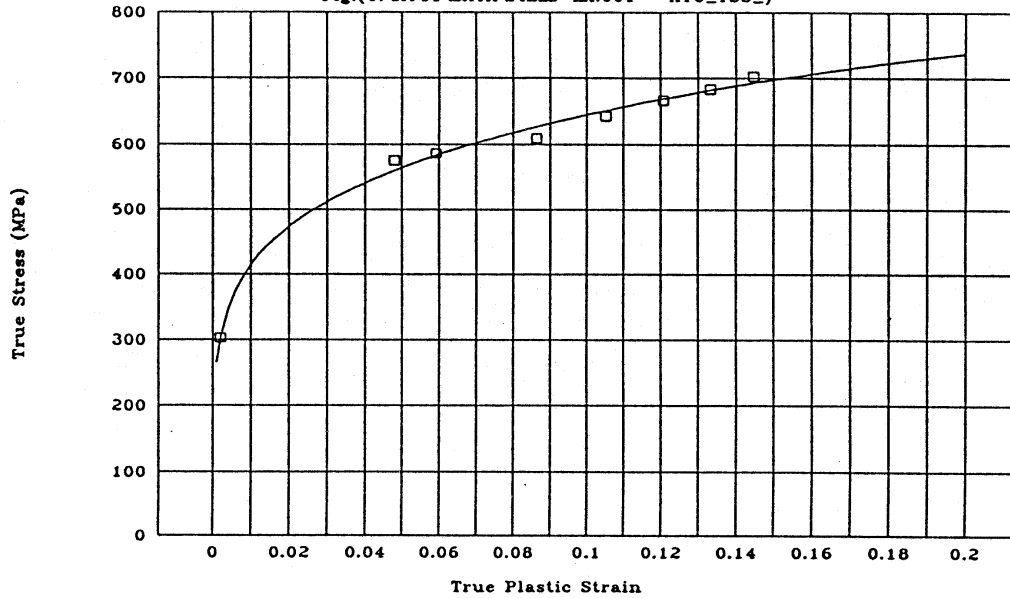
Fig.(C:\ATC\DATA\FIELD-EX.001 - ATC_DATA)



(a)

True-Stress/True-Plastic-Strain

Fig.(C:\ATC\DATA\FIELD-EX.001 - ATC_TSS_)



(b)

FIG. 2--In situ ABI test results of the heat-affected-zone (HAZ) in a circumferentially welded 347 stainless steel pipe (shown in Fig. 1) using a 1.57-mm-diameter tungsten carbide indenter: (a) indentation load-depth plot, (b) true-stress/true-plastic-strain data and curve fitting.

curve can be represented by the familiar power law equation:

$$\sigma_t = K \epsilon_p^n \quad (4)$$

where

n = strain-hardening exponent and K = strength coefficient

It should be noted that this representation is not a necessary requirement for determining the indentation-derived σ_t - ϵ_p data as will be shown later (equations 5 and 6) but it can be used to determine the strain-hardening exponent over the ϵ_p range of interest. Furthermore, a single power curve may not fit the entire σ_t - ϵ_p curve as noted in ASTM Test Method for Tensile Strain-Hardening Exponent (n-Values) of Metallic Sheet Materials (E 646-78).

A computer program is used to solve the following equations and to thereby determine the flow curve from the ABI data.

$$\epsilon_p = 0.2 d_p/D \quad (5)$$

$$\sigma_t = 4P/\pi d_p^2 \delta \quad (6)$$

where

$$d_p = \{0.5 CD [h_p^2 + (d_p/2)^2] / [h_p^2 + (d_p/2)^2 - h_p D]\}^{1/3} \quad (7)$$

$$C = 5.47P(1/E_1 + 1/E_2) \quad (8)$$

$$\delta = \begin{cases} 1.12 & \phi \leq 1 \\ 1.12 + \tau \ln \phi & 1 < \phi \leq 27 \\ \delta_{\max} & \phi > 27 \end{cases} \quad (9)$$

$$\phi = \epsilon_p E_2 / 0.43 \sigma_t \quad (10)$$

$$\delta_{\max} = 2.87 \alpha_m \quad (11)$$

$$\tau = (\delta_{\max} - 1.12) / \ln(27) \quad (12)$$

In the above equations, σ_t is the true stress, ϵ_p is the true-plastic-strain, d_p is the plastic indentation diameter, D is the diameter of the ball indenter, P is the applied indentation load, h_p is the plastic indentation depth, E_1 is the elastic modulus of the indenter, E_2 is the elastic modulus of the test material, δ is a parameter whose value depends on the stage of development of the plastic zone beneath the indenter, α_m is a parameter proportional to the strain rate sensitivity of the test material or specimen (e.g., for low strain-rate-sensitive materials $\alpha_m = 1.0$), and "ln" is the natural logarithm.

The engineering ultimate strength (UTS) can be calculated from the ABI test results (if the material stress-strain curve follows a power law) as follows:

$$\text{UTS} = K \cdot (n/e)^n \quad (13)$$

Brinell Hardness

The Brinell hardness number (HB) can also be determined from the ABI test using the maximum indentation load (P_{\max} in Kgf) and the final impression diameter (d_f in mm) and the indenter diameter (D in mm) using the following equation (Standard Test Method for Brinell Hardness of Metallic Materials, ASTM E 10-84):

$$HB = 2P_{\max} / [\pi D(D - (D^2 - d_f^2)^{0.5})] \quad (14)$$

Fracture Toughness

A simple technique is described [2,3,5] for estimating the fracture toughness by coupling the ABI-measured flow properties with a modified but empirically calibrated critical fracture strain model. This technique is currently limited to ductile fracture applications. The critical fracture strain model for ductile fracture prediction can be expressed in the following form [16,17]

$$K_{JIC} = \text{Constant} (\epsilon_f^* \cdot \ell_o^* \cdot E \cdot \sigma_y)^{0.5} \quad (15)$$

where K_{JIC} is the initiation fracture toughness calculated from J_{Ic} , ϵ_f^* is the critical fracture strain, ℓ_o^* is the characteristic distance ahead of the crack tip over which the strain must exceed ϵ_f^* , E is the elastic modulus, and σ_y is the yield strength. The modification [18] of this model involved: (1) the use of measured uniform strain from tensile tests or the strain-hardening exponent from ABI tests instead of the critical fracture strain value required in the original model, and (2) the assumption of an empirically calibrated value for the characteristic distance, ℓ_o^* , for each class of material. The determination of the critical fracture strain, ϵ_f^* , requires testing of several circumferentially notched round tensile specimens each having a different value of its notch root radius. Since this approach is costly, values of the critical fracture strain, ϵ_f^* , were not determined for the materials used in this work and "n" values were used instead.

The modified critical strain model can now be written as:

$$K_{JIC} = \text{Constant} (n \cdot \ell_o^* \cdot E \cdot \sigma_y)^{0.5} \quad (16)$$

The characteristic distance, ℓ_o^* , for ductile fracture is usually a multiple of the inter-particle spacing and currently it should be regarded as essentially an empirically obtained quantity. Although this dimension is presumably of relevance to the microstructural aspects of fracture initiation it is plausibly related to the yield strength, strain-hardening exponent (a measure of work-hardening), and the strength coefficient of the test material. However, more research is needed to better quantify and define this dimension in order to be able to use this method of estimating fracture toughness for applications where this characteristic distance is expected to change (e.g. due to radiation embrittlement).

A new empirical model, used successfully [2] for estimating the fracture toughness in A508 class 4 forging, is described by the following equation:

$$K_{JIC} = \text{Constant} (K \cdot d \cdot n \cdot \sigma_y)^{0.5} \quad (17)$$

where d is the grain size of the test material, K is the strength coefficient, n is the strain hardening exponent, and σ_y is the yield strength. The remaining constant needs to be determined and verified by correlations with more extensive data. This model eliminates the need for the characteristic distance and uses three parameters measured from ABI tests (namely, σ_y , K , and n). Furthermore, the grain size could be determined, nondestructively, in the field for structural components using portable metallography equipment. However, more fracture toughness and ABI measurements are needed to quantify the applicability of this model to many heats of materials.

RESULTS AND DISCUSSION

In Situ ABI Testing of Structural Components

A flat 347 stainless steel (SS) specimen obtained from an aerospace alloy (Heat No. F846) was tested prior to testing the 347 SS pipe to establish a comparison between ABI and tensile test results. The ABI-measured yield strength of 315.8 MPa (from one 7-cycles test) was in good agreement with the tensile yield strength of 317.2 MPa (indicated on this material's test report). A total of five ABI tests were then performed on the 100 mm outer diameter 347 SS pipe (5 mm thick) containing a circumferential weld (308 SS). The testing head of the portable/*in situ* stress-strain microprobe system was clamped on the pipe using four 90° V-blocks as shown in Fig. 1. This mounting method allowed the testing head to be rotated 360° and clamped rigidly for ABI testing at any location of the weld, HAZ, or the base metal. A value of $\beta_m = 0.191$ (Ref. [2]) was used for all ABI tests on stainless steel samples and pipe materials. An example of the *in situ* ABI test results from the welded 347 SS pipe is shown in Fig. 2 and the results are summarized in Table 1 below. These ABI test results show that the flow properties measured by the microprobe at three circumferential weld areas are in good agreement with each other and are consistently slightly lower than those at the base metal and the HAZ test locations. The above *in situ* tests also successfully demonstrate the potential applicability of the microprobe system to nondestructively test welded pipes and pressure vessels in the petroleum, fossil and nuclear power plants, etc.

ABI Testing of Welds and Irradiated Materials

The bench-top configuration of the stress-strain microprobe was used in testing laboratory specimens of a double-V weld from a high strength steel. The ABI test results at three test locations - base metal (BM), heat-affected-zone (HAZ), and weld metal (Weld)- are shown in Fig. 3. This figure shows that the flow properties (true-stress/true-plastic-strain curve) of the HAZ is not necessarily bracketed by those from the BM and Weld on both sides of the HAZ material. It might be higher (Fig. 3) or lower than both of them (as seen in other

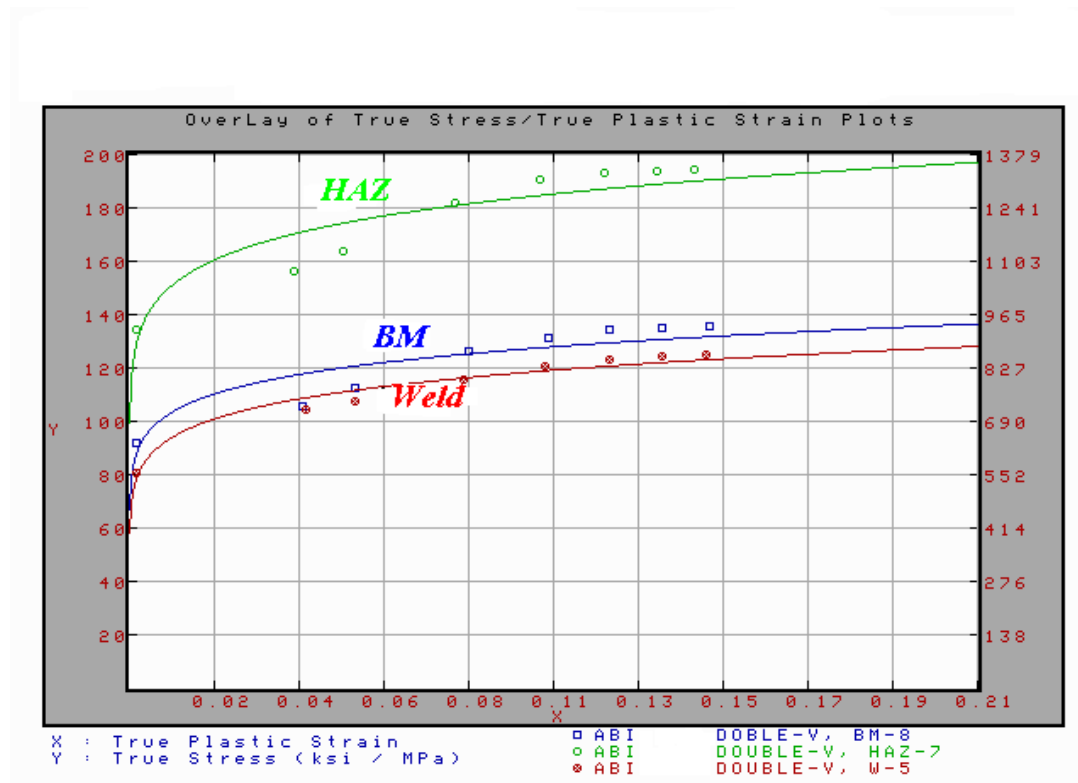
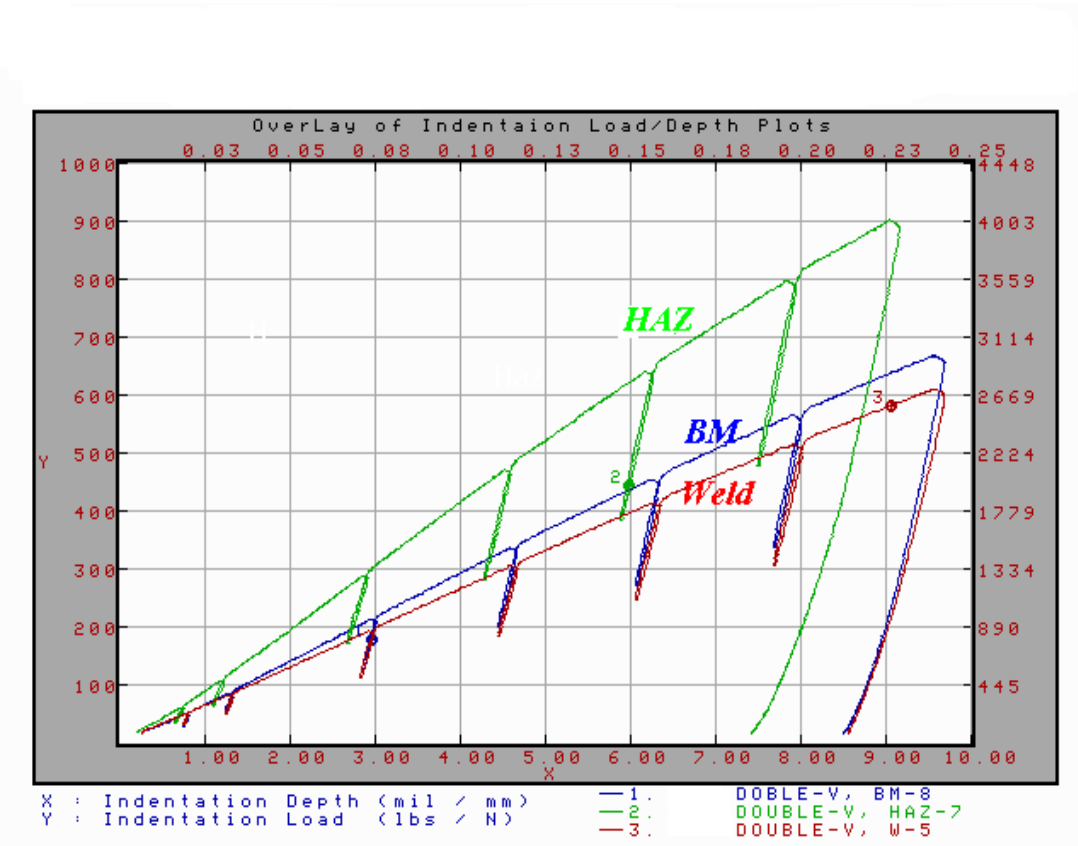


FIG. 3--Comparison of ABI test results on base metal (*BM*), heat-affected-zone (*HAZ*), and weld metal (*Weld*) in a double-V weld of a high carbon steel.

TABLE 1-Summary of *In Situ* ABI test results from welded 347 SS pipe.

Test Area	ABI-True Stress/ True-Plastic Strain (Equation)	ABI-Yield Strength (MPa)	Ultimate Strength (MPa)	Brinell Hardness
<u>Weld Metal (308 SS):</u>				
Test No. 1	σ_t (MPa) = 990 ϵ_p ^{.198}	283	589	169
Test No. 2	σ_t (MPa) = 920 ϵ_p ^{.190}	283	555	164
Test No. 3	σ_t (MPa) = 971 ϵ_p ^{.190}	300	586	172
<u>HAZ:</u>				
Test No. 4	σ_t (MPa) = 1060 ϵ_p ^{.191}	331	638	186
<u>Base Metal (347 SS):</u>				
Test No. 5	σ_t (MPa) = 1097 ϵ_p ^{.197}	325	654	188

ABI tests not in this paper). The nondestructive aspect of the ABI technique allows testing welded joints without the need to destructively machine miniature specimens which might also release residual stresses (generated from the welding procedure). Furthermore, the localized ABI testing allows testing very narrow and/or irregular geometry HAZ areas. The SSM system can be used to map out gradients in the stress-strain behavior of welded structural components nondestructively *in situ*. Hence, structural integrity and/or proper welding procedures and post-weld heat treatments can be evaluated.

The ABI technique was used to assess the degree of neutron-embrittlement damage and the percentage ductility recovery due to post-irradiation thermal annealing. To establish a reference condition, ABI tests were conducted on the end tabs of broken, flat, miniature, tensile specimens of A533B-1 pressure vessel steel. Both tensile and ABI tests were conducted using the same SSM system. Excellent agreement between stress-strain curves from both ABI and tensile tests is shown in Fig. 4. The ABI-measured stress-strain curves (Fig 5) show that the 343°C/168h thermal annealing resulted in a partial recovery while the thermal annealing at 454°C/168h resulted in full recovery of mechanical properties of the irradiated A533B [Heavy Section Steel Technology (HSST) Plate 02]. This was consistent with the results from destructive fracture toughness and Charpy impact tests [21]. The results shown in Fig. 5 demonstrate the capability of the SSM system to quantify the degree of embrittlement and recovery due to mitigation procedures of nuclear reactor pressure vessel steels. Furthermore, the SSM system can also monitor, nondestructively *in situ*, the re-embrittlement rate of nuclear pressure vessels following their thermal annealing during their life-extension.

CONCLUSIONS

- (1) The ABI technique of the SSM system was successful in accurately determining the yield strength and measuring the flow properties of welds in several metallic materials and

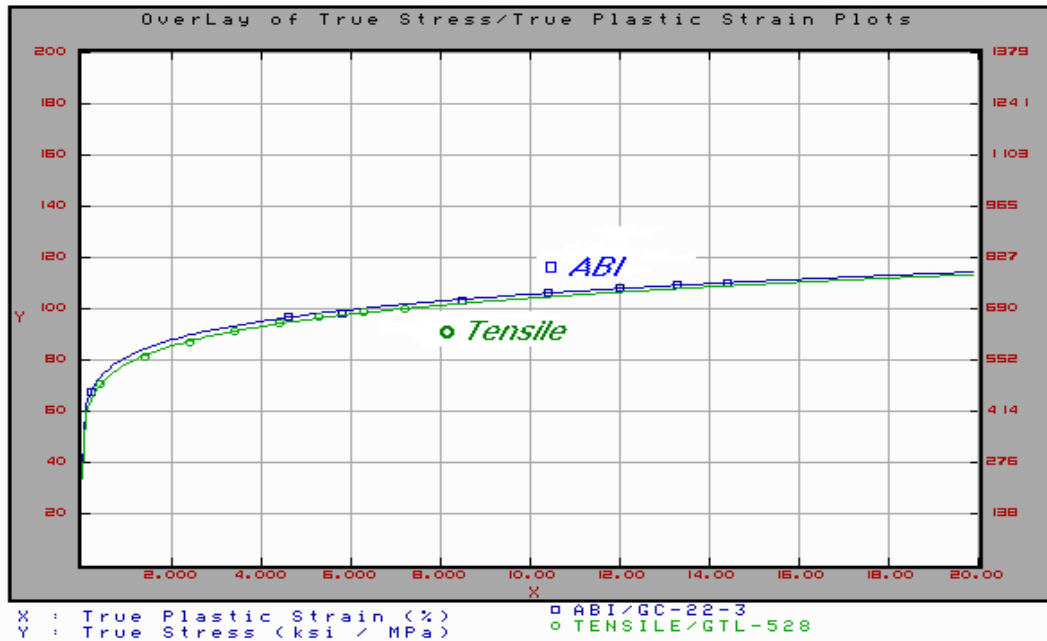


FIG. 4--Comparison between true-stress/true-plastic-strain curves obtained from ABI and tensile tests on A533B-1 pressure vessel steel.

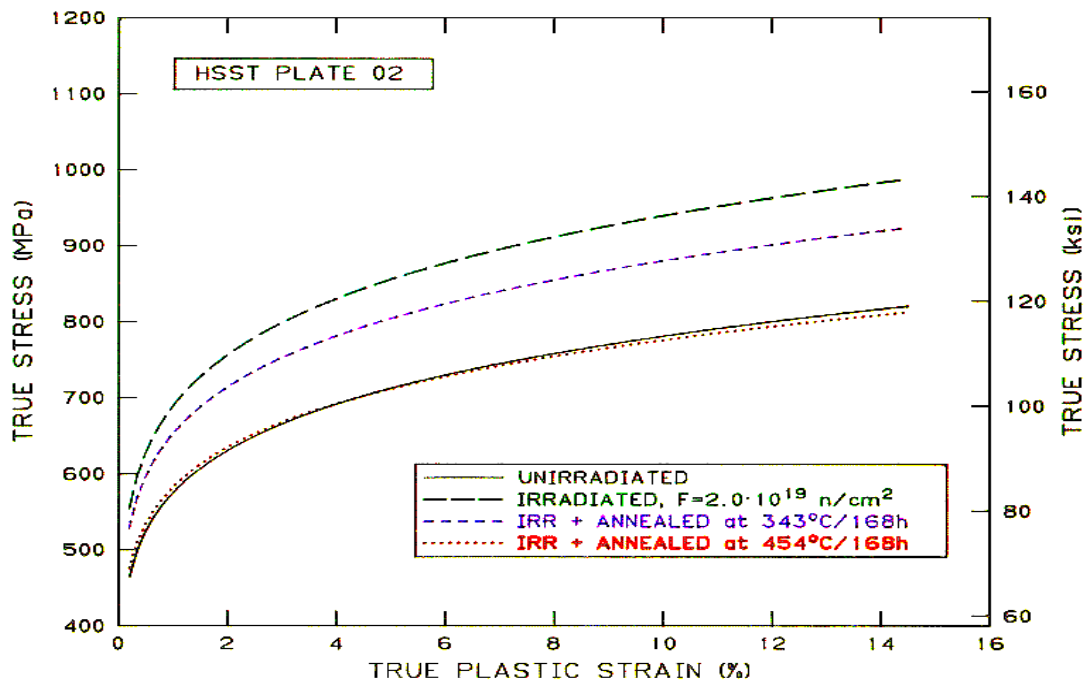


FIG. 5--Stress-strain curves from ABI tests on A533-B1 (HSST Plate 02) in four conditions, i.e. unirradiated, neutron-irradiated (embrittled), and two post-irradiated thermally-annealed conditions (to mitigate its radiation damage).

structural components. The gradients in mechanical properties of weld metals and their HAZs were successfully determined from ABI tests conducted on both laboratory specimens as well as on structural components.

(2) The SSM system quantified the degree of neutron-embrittlement damage as well as the percentage recovery in mechanical properties resulting from post-irradiation thermal annealing of nuclear pressure vessel steels.

(3) The *in situ* nondestructive capability of the SSM system can be used to monitor the aging of bridges and other critical components and to verify their structural integrity. Furthermore, welding and repair procedures can be accurately assessed.

REFERENCES

- [1] Haggag, F. M., "Field Indentation Microprobe for Structural Integrity Evaluation," U.S. Patent No. 4,852,397, August 1, 1989.
- [2] Haggag, F. M., "In-Situ Measurements of Mechanical Properties Using Novel Automated Ball Indentation System," Small Specimen Test Techniques Applied to Nuclear Reactor Thermal Annealing and Plant Life Extension, ASTM STP 1204, W. R. Corwin, F. M. Haggag, and W. L. Server, Eds., American Society for Testing and Materials, Philadelphia, 1993, pp. 27-44.
- [3] Haggag, F. M., Nanstad, R. K., Hutton, J. T., Thomas, D. L., and Swain, R. L., "Use of Automated Ball Indentation Testing to Measure Flow Properties and Estimate Fracture Toughness in Metallic Materials," Applications of Automation Technology to Fatigue and Fracture Testing, ASTM STP 1092, A. A. Braun, N. E. Ashbaugh, and F. M. Smith, Eds., American Society for Testing and Materials, Philadelphia, 1990, pp. 188-208.
- [4] Haggag, F. M., Nanstad, R. K., and Braski, D. N., "Structural Integrity Evaluation Based on an Innovative Field Indentation Microprobe," pp. 101-107 in Innovative Approaches to Irradiation Damage and Failure Analysis, D. L. Marriott, T. R. Mager, and W. H. Bamford, Eds., PVP Vol. 170, American Society of Mechanical Engineers, New York, 1989.
- [5] Haggag, F. M. and Nanstad, R. K., "Estimating Fracture Toughness Using Tension or Ball Indentation Tests and a Modified Critical Strain Model," pp. 41-46 in Innovative Approaches to Irradiation Damage and Failure Analysis, D. L. Marriott, T. R. Mager, and W. H. Bamford, Eds., PVP Vol. 170, American Society of Mechanical Engineers, New York, 1989.
- [6] Haggag, F. M., Wong, H., Alexander, D. J., and Nanstad, R. K., "The Use of Field Indentation Microprobe in Measuring Mechanical Properties of Welds," Recent Trends in Welding Science and Technology, TWR'89, Proceedings of the 2nd

International Conference on Trends in Welding Research, Gatlinburg, Tennessee, U.S.A., 14-18 May, 1989, pp. 843-849, 1990.

- [7] Haggag, F. M., "Application of Flow Properties Microprobe to Evaluate Gradients in Weldment Properties", International Trends in Welding Sciences and Technology, S.A. David and J. M. Vitek, Eds., ASM, Metals Park, Ohio, 1993, pp.629-635.
- [8] Haggag, F. M. and Bell, G. E. C., "Measurement of Yield Strength and Flow Properties in Spot Welds and Their HAZs at Various Strain Rates," International Trends in Welding Sciences and Technology, S.A. David and J. M. Vitek, Eds., ASM, Metals Park, Ohio, 1993, pp.637-642.
- [9] Haggag, F. M., "The Role of Lüders Strain in Predicting Flow Properties in Steels from an Instrumented Hardness Test," M.S. Thesis, Department of Chemical and Nuclear Engineering, University of California, Santa Barbara, California, 1980.
- [10] Haggag, F. M. and Lucas, G. E., "Determination of Lüders Strains and Flow Properties in Steels from Hardness/Microhardness Tests," Metallurgical Transactions A, 14A, 1983, pp.1607-1613.
- [11] Au, P., Lucas, G. E., Shekherd, J. W., and Odette, G. R., "Flow Property Measurements from Instrumented Hardness Tests," Non-destructive Evaluation in the Nuclear Industry, Metals Park, OH., 1980, pp. 597-610.
- [12] Tabor, D., "The Hardness of Metals," Clarendon Press, Oxford, 1951.
- [13] Francis, H. A., "Phenomenological Analysis of Plastic Spherical Indentations," Transactions of the ASME, July 1976, pp. 272-281.
- [14] George, R. A., Dinda, S., and Kasper, A. S., "Estimating Yield Strength from Hardness Data", Metal Progress, May 1976, pp. 30-35.
- [15] Server, W. L. and Oldfield, W., "Nuclear Pressure Vessel Steel Data Base," EPRI Report NP-933, 1978.
- [16] Pandey, R. K., and Banerjee, S., "Strain Induced Fracture in Low Strength Steels," Engineering Fracture Mechanics, Vol. 10, 1978, pp. 817-29.
- [17] Ritchie, R. O., Server, W. L., and Waullaert, R. A., "Critical Fracture Stress and Fracture Strain Models for Prediction of Lower and Upper Shelf Toughness in Nuclear Pressure Vessel Steels," Metallurgical Transactions. A, Vol 10A, 1979, pp. 1557-70
- [18] Haggag, F. M., Reuter, W. G., and Server, W. L., "Recovery of Fracture Toughness of Irradiated Type 347 Stainless Steel Due to Thermal Stress Relief: Metallographic and Fractographic Studies," Proceedings of the 2nd International Symposium on

Environmental Degradation of Materials in Nuclear Power Systems-Water Reactors, Monterey, California, September 9-12, 1985, 1986, pp. 509-14.

- [19] Pavinich, W. A., "The Effect of Neutron Fluence and Temperature on the Fracture Toughness and Tensile Properties for a Linde 80 Submerged Arc Weld," Proceedings of the 2nd International Symposium on Environmental Degradation of Materials in Nuclear Power Systems-Water Reactors, Monterey, California, September 9-12, 1985, 1986, pp. 485-95.
- [20] Haggag, F. M., Server, W. L., Lucas, G. E., Odette, G. R., and Shekherd, J. W., "The Use of Miniaturized Tests to Predict Flow Properties and Estimate Fracture Toughness in Deformed Steel Plates," Journal of Testing and Evaluation, JTEVA, Vol. 1, No. 1, Jan. 1990, pp. 62-69.
- [21] Mikhail A. Sokolov, Donald E. McCabe, Shafik K. Iskander, and Randy K. Nanstad, "Comparison of Fracture Toughness and Charpy Impact Properties Recovery by Thermal Annealing of Irradiated Reactor Pressure Vessel Steels," Seventh International Symposium on Environmental Degradation of Materials in Nuclear Power Systems - Water Reactors, Breckenridge, Colorado, August 7-10, 1995, 1995, pp. 771-782.